

Gating pore currents demonstrate selective and specific modulation of individual sodium channel voltage sensors by biological toxins. Xiao, Blumenthal and Cummins. *Molecular Pharmacology*

Supplemental Data

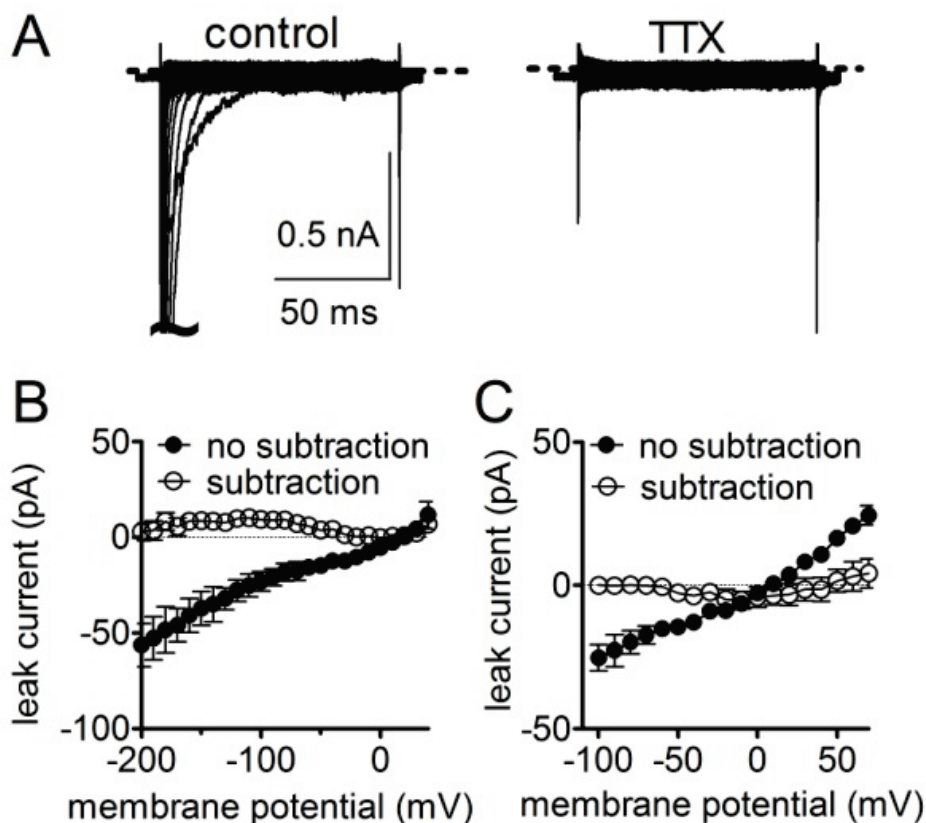
Gating pore currents demonstrate selective and specific modulation of individual sodium channel voltage sensors by biological toxins.

Yucheng Xiao, Kenneth Blumenthal and Theodore R. Cummins

Department of Pharmacology and Toxicology, Indiana University School of Medicine,
Indianapolis, Indiana 46202 (Y.X., T.R.C.),

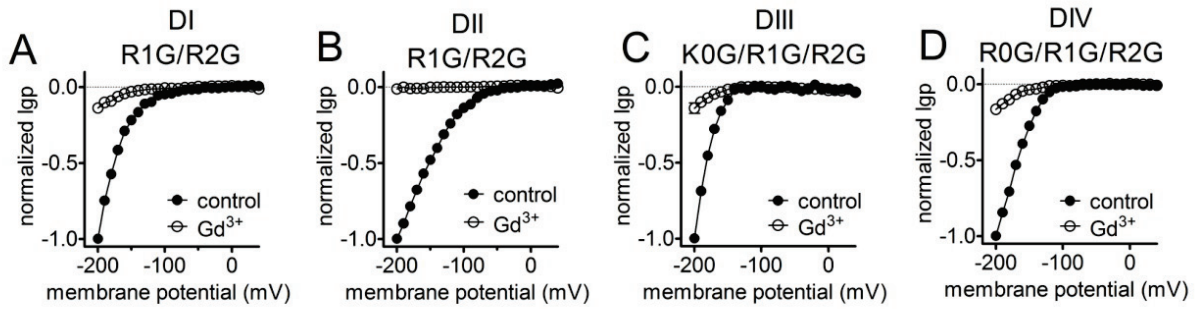
Department of Biochemistry, School of Medicine and Biomedical Sciences, State
University of New York, Buffalo, New York 14214, USA (K.B.)

Gating pore currents demonstrate selective and specific modulation of individual sodium channel voltage sensors by biological toxins. Xiao, Blumenthal and Cummins. *Molecular Pharmacology*



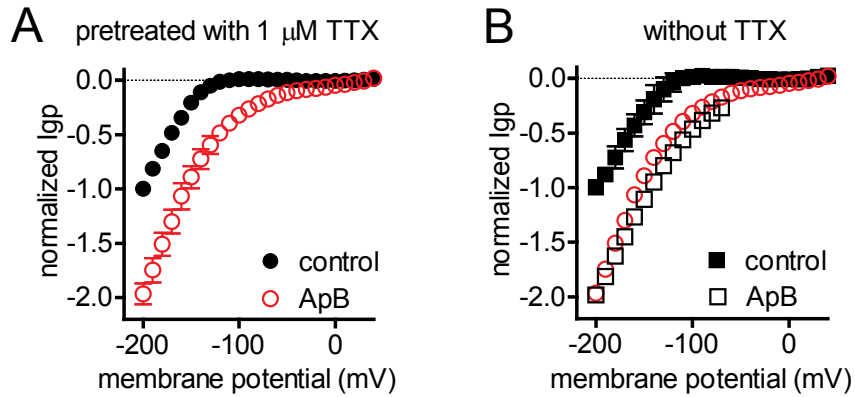
Supplemental Figure 1. No gating pore current (I_{gp}) was generated by WT* Nav1.5 expressed in HEK293 cells. (A), Typical current traces before (*left*) and after (*right*) application of 1 μ M TTX. Currents were elicited by applying 100-ms pulses from a holding potential of -100 mV to various potentials ranging from -200 to +70 mV in 10 mV increments. No linear leak and capacitance currents were subtracted. (B), The I-V curves of leak currents at voltages between -200 mV and +40 mV before (filled circles) and after (open circles) applying linear leak subtraction in the presence of 1 μ M TTX. The subtraction of linear leak currents was carried out by fitting the I-V response between 0 mV and 40 mV. (C), The I-V curves of leak current at voltages between -100 mV and +70 mV before (filled circles) and (open circles) linear leak subtraction in the presence of 1 μ M TTX. The subtraction of linear leak currents was carried out by fitting the I-V response between -100 mV and -60 mV. In both (B) and (C), the amplitude of currents was measured at a time point of between 90 – 100 ms after the start of the pulse. Note that a TTX- and HWTX-IV-sensitive hNav1.5 construct (C373Y/R800D/S802E) was referred to as WT*.

Gating pore currents demonstrate selective and specific modulation of individual sodium channel voltage sensors by biological toxins. Xiao, Blumenthal and Cummins. *Molecular Pharmacology*



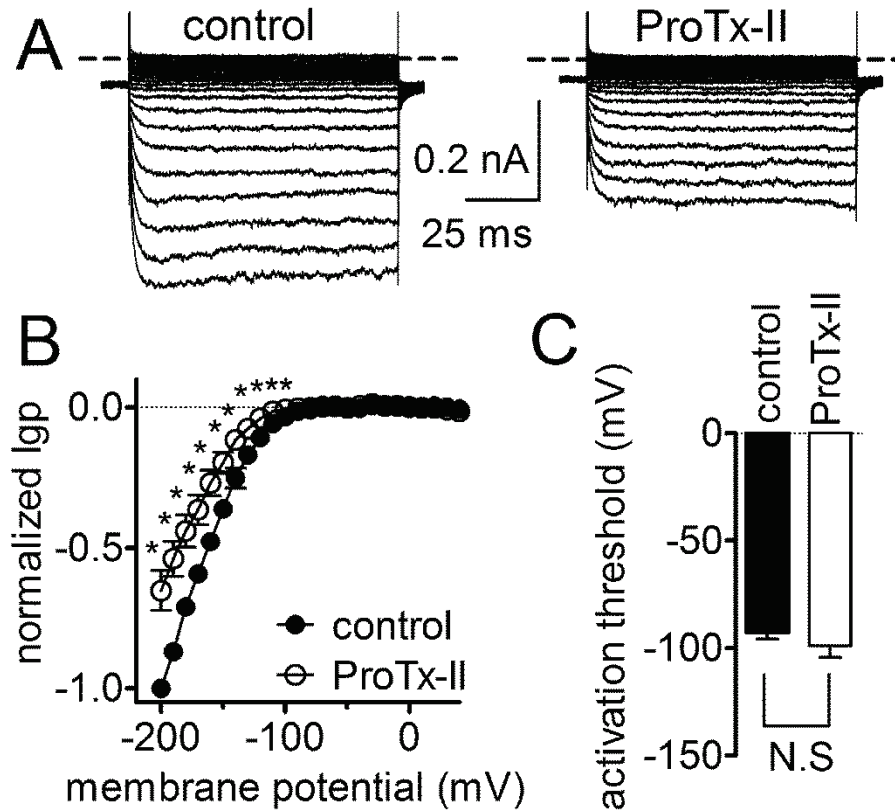
Supplemental Figure 2. Gd³⁺ inhibited inward I_{gp} fluxing through hNav1.5 DI - DIV voltage sensor mutants. Cells were held at -100 mV and pretreated with 1 μ M TTX. The subtraction of linear leak currents has been performed before (filled circles) and after application (open circles) of 1 mM Gd³⁺. I_{gp} were normalized to the maximal control I_{gp} amplitude.

Gating pore currents demonstrate selective and specific modulation of individual sodium channel voltage sensors by biological toxins. Xiao, Blumenthal and Cummins. *Molecular Pharmacology*



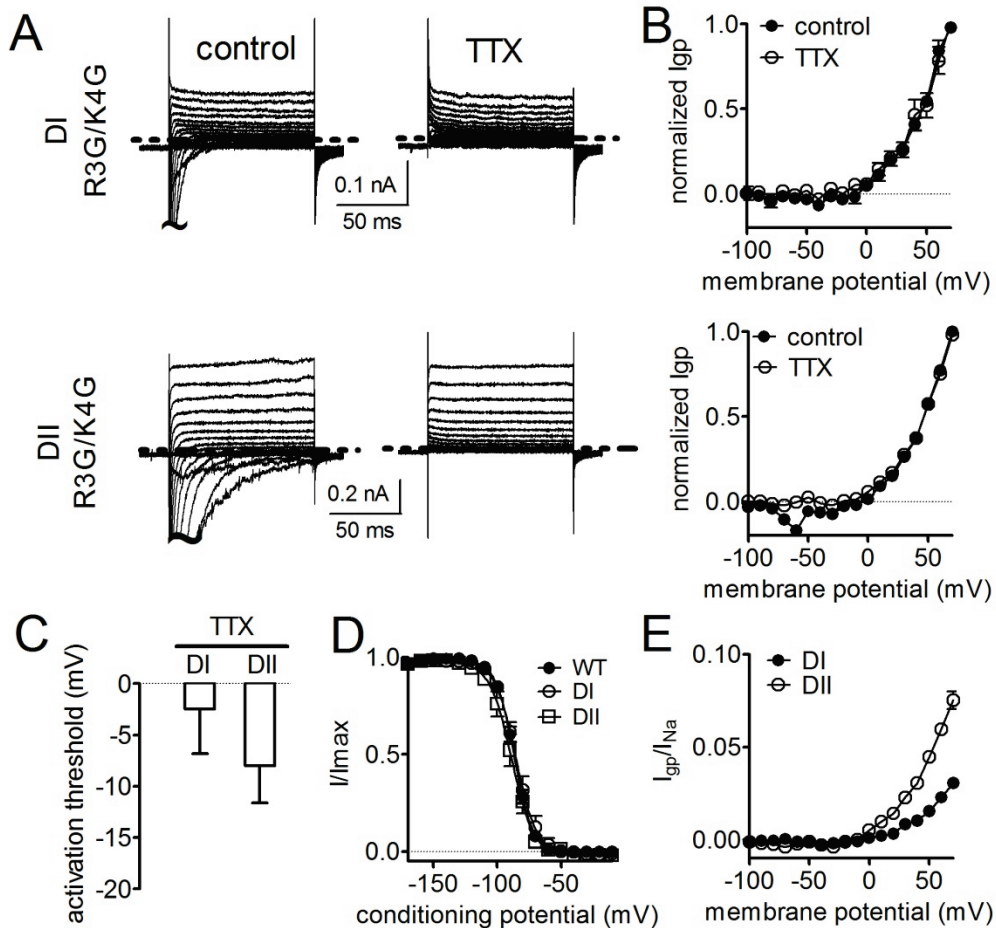
Supplementary Figure 3. Modification of DIV gating pore currents by ApB was not altered in the presence (A) or absence (B) of TTX. In (B), the data points for ApB-treated gating pore currents at voltages from -60 to +40 mV were not shown because the gating pore currents were contaminated by central pore current. ApB slowed down the fast inactivation of central pore current. The data points (red open circles) for ApB's effect in presence of 1 μM TTX in (B) were duplicated from (A). ApB concentration was 500 nM.

Gating pore currents demonstrate selective and specific modulation of individual sodium channel voltage sensors by biological toxins. Xiao, Blumenthal and Cummins. *Molecular Pharmacology*



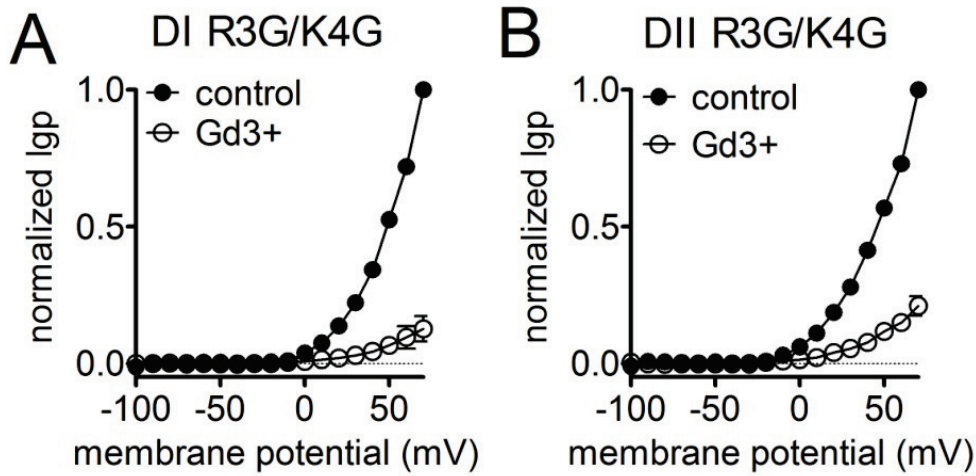
Supplemental Figure 4. ProTx-II modulates inward Igp generated by DIV VSD mutations in hNav1.7. Application of 1 μ M ProTx-II reduced the inward Igp through the DIV VSD of hNav1.7 (A). (B) The inhibition was observed at potentials between -200 and -100 mV and greater than that observed with hNav1.5 DIV Igp. In (A) – (D), the subtraction of linear leak currents had been carried out as described in the legend of Fig. 1C. (C), Application of 1 μ M ProTx-II did not alter the activation threshold of hNav1.7 DIV Igp. The DIV gating pore currents in hNav1.7 were induced by mutating the outer three arginines in the DIV S4 segment (R0G/R1G/R2G). N.S., no significance; *, P < 0.05.

Gating pore currents demonstrate selective and specific modulation of individual sodium channel voltage sensors by biological toxins. Xiao, Blumenthal and Cummins. *Molecular Pharmacology*



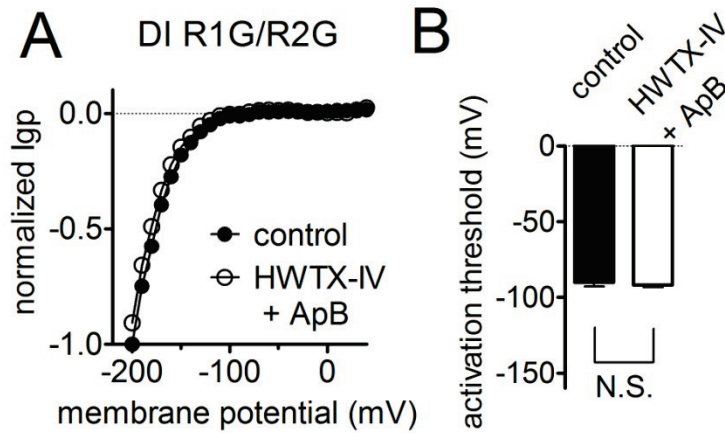
Supplemental Figure 5. Double Gly-mutations of the 3rd and 4th gating-charge residues in Nav1.5 DI and DII voltage sensors produced outward I_{gp} in HEK293 cells. Cells were held at -100 mV. (A), Typical current traces before (left) and after (right) application of 1 μ M TTX. All currents were elicited by 100-ms depolarizing steps to various potentials that ranged from -100 to +70 mV. No subtraction of linear leak and capacitance currents was performed. The dotted line across current traces represents the zero current level. Outward I_{gp} were normalized to the maximal control I_{gp} . (B), 1 μ M TTX failed to affect the I-V curves of outward I_{gp} through DI- or DII voltage sensor mutant. Note that the linear leak currents have been subtracted as described in the legend of Supplemental Figure 1C. (C), 1 μ M TTX did not significantly alter the activation thresholds of outward I_{gp} through DI or DII voltage sensor mutant. (D), Double mutations R3G/K4G in DI or DII voltage sensor did not significantly shift steady-state inactivation. Currents were induced by the same standard double protocol as described in the legend of Figure 2D. (E), Ratio of I_{gp} to the total I_{Na} at various potentials. The ratio of outward I_{gp} was estimated by the equation as described in the legend of Figure 2E. Note that all mutations of gating-charge residues were constructed based on WT* hNav1.5 channel. N.S., no significance.

Gating pore currents demonstrate selective and specific modulation of individual sodium channel voltage sensors by biological toxins. Xiao, Blumenthal and Cummins. *Molecular Pharmacology*



Supplemental Figure 6. Gd³⁺ inhibited the outward Igp fluxing through hNav1.5 DI (A) and DII (B) voltage sensor mutants. Cells were held at -100 mV and pretreated with 1 μ M TTX. In (A) and (B), outward Igp were induced by 100-ms depolarizing steps to various potentials that ranged from -100 to +70 mV. The linear leak currents were subtracted as described in the legend of Supplemental Figure 1C. Gd³⁺ concentration is 1 mM.

Gating pore currents demonstrate selective and specific modulation of individual sodium channel voltage sensors by biological toxins. Xiao, Blumenthal and Cummins. *Molecular Pharmacology*



Supplemental Figure 7. Effect of the HWTX-IV + ApB mixture on inward Igp generated by hNav1.5 DI voltage sensor mutant (R1G/R2G). (A), Effect of toxin mixture on the I-V curve of inward Igp fluxing through DI voltage sensor mutant. Inward Igp were elicited by the protocol as described in the legend of Supplemental Figure 3. Cells were held at -100 mV and pretreated with 1 μ M TTX. The subtraction of linear leak currents has been performed. All currents are normalized to the maximal control current amplitude. (B), Effect of toxin mixture on the activation threshold of inward Igp. Note that the double Gly-mutation of R1/R2 in DI was constructed based on WT* Nav1.5 channel. Toxin mixture: 1 μ M HWTX-IV and 100 nM ApB. N.S., no significance.